# Loss of SORCS2 is associated with neuronal DNA double-strand breaks

Katerina O. Gospodinova[1], Ditte Olsen[2], Mathias Kaas[2], Susan M. Anderson[1], Jonathan Phillips[1], Rosie M. Walker[1,3], Mairead L. Bermingham[1], Abigail L. Payne[1], Panagiotis Giannopoulos[1], Divya Pandya[1], Tara L. Spires-Jones[4], Catherine M. Abbott[1], David J. Porteous[1], Simon Glerup[2], Kathryn L. Evans[1]

1. Centre for Genomic and Experimental Medicine, University of Edinburgh, Edinburgh, EH4 2XU, UK

2. Department of Biomedicine, Aarhus University, Aarhus, 8000, Denmark

3. Chancellor's Building, 49 University of Edinburgh, Edinburgh, EH16 4SB, UK (current address)

4. Centre for Discovery Brain Sciences, UK Dementia Research Institute, University of Edinburgh, Edinburgh, EH8 9XD, UK

Katerina O. Gospodinova: kgospodi@exseed.ed.ac.uk ; Ditte Olsen: olsen@biomed.au.dk; Mathias Kaas mko@biomed.au.dk; Susan M. Anderson S.M.Anderson@ed.ac.uk; Jonathan Phillips Jonathan.Phillips@ed.ac.uk; Rosie M. Walker: rwalke13@staffmail.ed.ac.uk; Mairead L. Bermingham: mairead.bermingham@ed.ac.uk; Abigail L. Payne: abbiepayne22@hotmail.com; Panagiotis Giannopoulos: s1582089@ed.ac.uk; Divya Pandya: divyapandya@hotmail.co.uk; Tara L. Spires-Jones: tara.spires-jones@ed.ac.uk; Catherine M. Abbott: c.abbott@ed.ac.uk; David J. Porteous: david.porteous@ed.ac.uk; Simon Glerup: glerup@biomed.au.dk; Kathryn L. Evans: Kathy.Evans@ed.ac.uk

Corresponding Author: Kathryn L. Evans, Centre for Genomic and Experimental Medicine, University of Edinburgh, Edinburgh, EH4 2XU, UK +44 131 651 8747

## Abstract

SORCS2 is one of five proteins that constitute the Vps10p-domain receptor family. Members of this family play important roles in cellular processes linked to neuronal survival, differentiation and function. Genetic and functional studies implicate SORCS2 in cognitive function, as well as in neurodegenerative and psychiatric disorders. DNA damage and DNA repair deficits are linked to ageing and neurodegeneration, and transient neuronal DNA double-strand breaks (DSBs) also occur as a result of neuronal activity. Here, we report a novel role for SORCS2 in DSB formation. We show that SorCS2 loss is associated with elevated DSB levels in the mouse dentate gyrus and that knocking out *SORCS2* in a human neuronal cell line increased Topoisomerase IIβ-dependent DSB formation and reduced neuronal viability. Neuronal stimulation had no impact on levels of DNA damage, suggesting that the observed differences are unlikely to be the result of aberrant neuronal activity. Our findings are consistent with studies linking the VPS10 receptors and DNA damage to neurodegenerative conditions.

## Key words

SORCS2, DNA double-strand breaks, neuronal activity, neurodegeneration

## Declarations

## Funding

This work was supported by University of Edinburgh internal funds in the form of a PhD studentship, grants from Alzheimer's Research UK (ARUK-PPG2019B-015 and ARUK-NC2019-SCO) and by the UK Dementia Research Institute, which receives its funding from UK DRI Ltd funded by the UK Medical Research Council, Alzheimer's Society and Alzheimer's Research UK, and the European Research

Council (ERC) under the European Union's Horizon 2020 research and innovation programme (Grant agreement No. 681181).

## Competing interests

Although not related to the present study, SG is a shareholder of Muna Therapeutics and Teitur Trophics, both involved in developing therapies directed at SorCS2. The remaining authors declare that they have no competing interests.

## Availability of data and materials

Please contact author for data requests.

## Code availability

Not applicable.

## Authors' contributions

KOG and KLE conceived and planned the experiments. KOG performed the majority of the experiments and data analysis. SG provided the mice and DO and MK performed the behavioural experiments. SMA, JP, AP, PG and DP contributed to the execution of the experiments. RMW and MLB performed the statistical analysis of the mouse data. TSJ provided materials and support during assay optimisation. SG, CMA, TSJ and DJP contributed through strategic discussions. KOG and KLE wrote the manuscript with input from all authors.

## Ethics approval

All experiments were approved by the Danish Animal Experiments Inspectorate under the Ministry of Justice (Permits 2011/561-119, 2016-15-0201-01127 and 2017-15-0201-01192) and carried out according to the ARRIVE guidelines.

## Consent to participate

Not applicable.

**Consent for publication**

Not applicable.

## Introduction

SORCS2 is a member of the VPS10p-domain receptor, or sortilin, family. The family comprises five multifunctional neuronal receptors: sortilin; SORLA and SORCS1-3, which are characterised by possession of a vacuolar protein sorting (VPS) 10p domain(Hermey 2009). All family members are involved in intracellular sorting and trafficking of various neurotrophic factors, transmembrane receptors and synaptic proteins, linking them to a broad range of cellular processes, including neuronal function, differentiation and synaptic plasticity(Glerup et al 2014a).

Genetic and functional analyses implicate the VPS10p-domain receptors in cognitive functions and a wide range of neurodegenerative and psychiatric disorders. Interrogation of the GWAS catalog (https://www.ebi.ac.uk/gwas/) indicates that multiple SNPs in *SORCS2* are involved in epistatic interactions that are associated ($p \leq 5x10^{-8}$) with paired helical filament tau (PHF-tau) levels (Wang et al 2020).Genetic variants in *SORCS2* are also significantly associated ($p \leq 5x10^{-8}$) with alcohol withdrawal (Smith et al 2018) and risk-taking behaviour (Karlsson Linnér et al 2019). In addition, there are suggestive associations ($5x10^{-8} < p < 1x10^{-5}$) with ADHD (Alemany et al 2015), anorexia nervosa (Duncan et al 2017), response to antidepressants (Fabbri et al 2018), depressive and manic episodes in bipolar disorder (Fabbri and Serretti 2016), memory performance (Greenwood et al 2019), and intelligence (Davies et al 2018). Elevated *SORCS2* levels have been detected in the brains of epileptic patients, as well as in the hippocampi of wild-type mice subjected to pentylenetetrazole (PTZ)-induced kindling, a model of epilepsy (Malik et al 2019). Meanwhile, application of PTZ-induced kindling in animals lacking *Sorcs2* increased the levels of oxidative stress and led to an exacerbated oxidative stress response in primary neurons (Malik et al 2019). Increased *SORCS2* expression has also been observed in response to application of the cortisol analogue, dexamethasone (DEXA), as well as following alcohol exposure in a human neuroblastoma cell line (Smith et al 2018). In mice, loss of *Sorcs2* has been linked to a decreased phenotypic preference for

112 alcohol and decreased alcohol withdrawal symptoms (Olsen et al 2019), suggesting a general role of
113 the receptor in the cellular and behavioural response to multiple stressors.

114 During mouse development (E15.5), *Sorcs2* is expressed in the ventral hippocampus and in tyrosine-
115 hydroxylase-positive (TH+) neurons of the midbrain. In the adult mouse brain, *Sorcs2* is strongly
116 expressed in hippocampal, striatal and cortical neurons (Deinhardt et al 2011; Glerup et al 2014b;
117 Glerup et al 2016). At the cellular level, in the hippocampus SorCS2 is located at the post-synaptic
118 density (PSD) of dendrites and within synaptic vesicles (Glerup et al 2016; Ma et al 2017). Through its
119 interactions with the BDNF receptor tyrosine kinase, TrkB, and the pro-BDNF receptor $p75^{NTR}$, it is
120 implicated in the induction of NMDA-dependent long-term potentiation (LTP) and depression (LTD)
121 in the hippocampus, respectively (Glerup et al 2016). Moreover, SorCS2 traffics TrkB to the PSD in an
122 activity-dependent manner, thus playing a role in synaptic tagging and synaptic potentiation
123 maintenance (Glerup et al 2016). The receptor has been also implicated in the trafficking of NMDA
124 receptor subunits to dendritic and synaptic surfaces in medium spiny neurons of the striatum (Ma et
125 al 2017) and in pyramidal neurons of the CA2 (Ma et al 2017; Yang et al 2020). In keeping with the
126 above findings, *Sorcs2*$^{-/-}$ mice exhibit learning and memory deficits (Glerup et al 2016) and
127 hyperactive behaviour on exposure to novelty (Olsen et al 2021).

128 DNA double-strand break (DSB) formation has been previously hypothesised to be involved in
129 learning and memory in wild-type mice via a behavioural task that involved exploration of a novel
130 environment (Suberbielle et al 2013; Madabhushi et al 2015). Suberbielle *et al.* (2013) (Suberbielle et
131 al 2013) reported the somewhat surprising finding of increased DSB formation in the hippocampus
132 and parietal cortex of adult wild-type mice following exploration of a novel environment. DSBs were
133 most abundant in the DG, an important area for learning and memory. The breaks were repaired
134 within 24 hours leading the authors to suggest that transient break formation plays a role in
135 chromatin remodelling and regulation of gene expression necessary for learning and memory
136 formation. Further experiments involving direct activation of the visual cortex and the striatum via

exposure to visual stimuli or optogenetic stimulation, respectively, showed that increases in neuronal activity in the absence of the behavioural paradigm were sufficient for inducing DSBs. Subsequent work by others showed that neuronal activity *in vivo* (induced via a contextual fear conditioning training paradigm) and *in vitro* also resulted in higher levels of DSBs than was seen in controls (Madabhushi et al 2015). Neuronal activity-induced DSBs were found to be located in the promoters of a subset of early-response genes and mediated by the type II topoisomerase, Topoisomerase IIβ (Topo IIβ): knockdown of Topo IIβ attenuated both DSB formation and early-response gene expression following neuronal stimulation (Madabhushi et al 2015). In keeping with these findings, *in vitro* pharmacological stimulation of neuronal activity has been shown to be associated with increased DSB formation (Suberbielle et al 2013; Madabhushi et al 2015).

Given the changes in synaptic plasticity and the altered response to novelty and to stress observed in the *Sorcs2*$^{-/-}$ mice, we hypothesised that loss of the receptor may lead to alterations in the number of DNA DSBs at baseline, following exploration of a novel environment and/or following a recovery period. In keeping with previous data, we detected an increase in DSB formation in the hippocampus of wild-type mice following exploratory activity and repair of these breaks after a recovery period. Compared to wild-type mice, *Sorcs2* knock-out mice had higher levels of DSBs in the DG at baseline with no differences seen after the novel environment or on recovery. Next, we investigated whether this difference would also be observed in human neurons lacking SORCS2. We used CRISPR/Cas9 genome editing to delete the gene from Lund Human Mesencephalic (LUHMES) human neurons (Lotharius et al 2002; Scholz et al 2011). We found that neurons from *SORCS2* knock-out lines had more DNA DSBs and were characterised by decreased viability compared to wild-type lines. There was no difference in the number of breaks observed in wild-type and knock-out lines following stimulation of neuronal activity.

## Materials and Methods

## Compounds and antibodies

Primary antibodies used in this study: polyclonal sheep anti-SORCS2 (AF4238, R&D Systems), monoclonal mouse anti-γH2A.X (JBW301, Millipore) and polyclonal rabbit anti-53BP1 (NB100304, Novus Biologicals). Secondary antibodies: rabbit anti-mouse Immunoglobulins/HRP (P0260, Dako), rabbit anti-sheep Immunoglobulins/HRP (P0163, Dako), Alexa Fluor® 488 donkey anti-mouse IgG (H+L) (A21202, Thermo Scientific) and Alexa Fluor® 568 donkey anti-rabbit IgG (H+L) (A21207, Thermo Scientific). Etoposide was purchased from Sigma (E1383).

## Animals

Mice were housed at the animal facility at Aarhus University, in groups of up to five mice per cage with a 12-h light/12-h dark schedule and fed standard chow (1324, Altromin) and water *ad libitum*. Cages were cleaned and supplied with bedding and nesting material every week. *Sorcs2*$^{-/-}$ mice had been backcrossed for ten generations into C57BL/6J Bomtac background (Glerup et al 2014b). All experiments were approved by the Danish Animal Experiments Inspectorate under the Ministry of Justice (Permits 2011/561-119, 2016-15-0201-01127 and 2017-15-0201-01192) and carried out according to the ARRIVE guidelines. Behavioural experiments were carried out using sex- and age-matched mice (male, 5-6 months old). Each of the behavioural tests described below were carried out using naïve animals in a randomized order by an investigator blinded to the mouse genotype. No animals were excluded from the subsequent analysis.

## Exploration of a novel environment

Mice in the control group (here defined as 'home cage') were kept in their original cages. Mice in the novel environment ('novel environment') and the recovery from the novel environment ('recovery') groups were transferred to the testing room, where they were individually exposed to a novel environment. The novel environment consisted of an Open Field Arena with four different novel objects and mint-like odour. Individual mice were allowed to explore the novel environment for 2h.

After the novel environment exploration, the mice in the novel environment group were sacrificed, while the mice in the recovery group were returned to their home cages, where they recovered from the behavioural task for 24h before being sacrificed. The mice from the home cage group were sacrificed at the same time point.

## Perfusion and tissue processing

Mice were perfused transcardially with cold PBS containing heparin (10,000 U/L), followed by ice-cold 4% paraformaldehyde (PFA) in phosphate-buffered saline (PBS). Whole brains were dissected and post-fixed overnight in 4% PFA in PBS. Following post-fixation, brains were rinsed in sterile PBS and cryoprotected first in 10% sucrose and then in 30% sucrose at 4°C until the tissue sank to the bottom of the tube. Brains were subsequently embedded in OCT compound on dry ice and stored at -80°C. Coronal sections (14µm thick) containing the brain areas of interest (i.e., DG at bregmas: -1.755, -2.155 and -2.555; CA2 and CA3 at bregmas: -1.755 and -2.1550) were obtained and mounted on Superfrost slides (Suppl. Fig. 1). Slides were stored at −80°C.

## LUHMES culture

LUHMES is a karyotypically normal human foetal mesencephalic cell line conditionally immortalised with the v-myc oncogene. Proliferation of the neuronal precursor cells can be terminated by adding tetracyclin, thus halting v-myc expression. Subsequent addition of GDNF results in robust differentiation into post-mitotic dopaminergic neurons within five days. LUHMES cells (ATCC, RRID: CVCL_B056) were grown and differentiated as described previously (Scholz et al 2011). Briefly, cell culture dishes were pre-coated with PLO (1mg/ml; P3655, Sigma) and fibronectin (1mg/ml; F1141, Sigma) in distilled $H_2O$ ($dH_2O$) for at least 3h at 37°C. Following incubation, the coating solution was aspirated, and plates/flasks were washed two times with $dH_2O$ and completely air dried before cell seeding. Prior to differentiation, LUHMES cells were maintained in proliferation medium consisting of Advanced DMEM/F12 (12634028, Life Technologies), L-glutamine (200mM; 25030081, Life Technologies), N2 supplement (100x; 17502-048, Life Technologies) and b-FGF (160µg/ml; 571502,

Biolegend). Experiments were conducted after 6 or 14 days of differentiation initiated by growing cells in differentiation media consisting of Advanced DMEM/F12, L-glutamine (200mM), N2 supplement (100x), cAMP (100mM; D0627, Sigma), Tetracycline hydrochloride (1mg/ml; T7660, Sigma) and recombinant human GDNF (20µg/ml; 212-GD-010, R&D).

CRISPR/Cas9 Genome Editing

Guide RNAs (gRNAs) targeting *SORCS2* exon 1 or exon 3 were designed using two independent online tools: the Zhang Lab CRISPR Design website (https://crispr.mit.edu) and CHOPCHOP (https://chopchop.cbu.uib.no/), and were selected based on their on/off-target activity. The oligos were phosphorylated and subsequently cloned into the px458 vector, co-expressing the Cas9 endonuclease and GFP (RRID: Addgene_48138). Low passage LUHMES cells were fed with fresh proliferating media 2h prior to transfection. Cells were dissociated using TrypLE (12605036, Thermo Scientific), counted and $2x10^6$ cells were transfected using the Basic Nucleofector kit for primary neurons (VAPI-1003, Lonza) and the D-33 programme on the Amaxa Nucleofector II B device (Amaxa Biosystems). 500µl of pre-warmed RPMI media (BE12-752F, Lonza) was added following nucleofection. The cells were then incubated at 37°C for 5min and gently added to precoated 6-well plates containing 2ml of freshly made proliferation medium. 2µg of the Cas9 plasmid containing the gRNA of interest were used in each transfection. Empty vector (EV) control lines were generated by transfecting proliferating LUHMES at an equivalent passage number with the px458 vector alone.

Forty-eight hours following transfection, cells were lifted as described before and centrifuged at 90g for 10min. The cell pellets were resuspended in 500µl of warm PBS and GFP+ cells were sorted by FACS into pre-coated 96-well plates, containing 100µl of freshly prepared proliferation medium. After seven days, 100µl of fresh proliferation medium was added to each well, and three days later single cell colonies were identified. At this stage, one third of the cells was kept for genotyping, and the rest were split into two wells of a 24-well plate for further expansion.

CRISPR/Cas9 sgRNAs and Primer Sequences

gRNA *SORCS2* exon 1: CGGAGTGGCTTCGCGGGCGC

gRNA *SORCS2* exon 3: CCGTCATCGACAATTTCTAC

*SORCS2* exon 1 Forward primer: CCTTTCTCTGCGCTCTCG

*SORCS2* exon 1 Reverse primer: CCGCCCCTGATGACCATA

*SORCS2* exon 3 Forward primer: CAGAGTGCCCAGGACTGTAC

*SORCS2* exon 3 Reverse primer: ATGTGCCCTAGGTATGCAGG

Western blotting

Cells were lysed in ice cold 1% Triton lysis buffer (20mM Tris-HCl pH 8.0, 10mM EDTA, 1% Triton X-100 and 1x protease inhibitor cocktail (5892970001, Roche) ) and protein concentration was measured using Bio-Rad BSA protein assay (5000116, Bio-Rad). Protein lysates were loaded on NuPAGE Tris-acetate 3-8% precast gels (EA03752BOX, Life Technologies) and ran at 150V for 1.5h. Gels were transferred onto PVDF membranes at 30V for 1.5h. Membranes were blocked in 5% milk in 0.2% Tween-20 in TBS for 1h at room temperature and probed with primary antibodies against SORCS2 (1:750; AF4238, R&D Systems) and GAPDH (1:10,000; MAB374, Merck) diluted in blocking solution overnight at 4°C. After washes (3x 10min) in 0.2% Tween-20 in TBS, membranes were incubated with secondary HRP-conjugated antibodies diluted 1:10,000 in blocking solution for 1h at room temperature. After another three washes with TBS-0.2% Tween-20, blots were visualised using the Pierce ECL Plus Western Blotting Substrate (11527271, Thermo Scientific) and exposed using autoradiography film.

Immunofluorescence staining

Slides containing brain sections were thawed at room temperature, incubated for 10min in 4% PFA in PBS and then thoroughly washed for 30min in PBS containing 100mM glycine (1042011000, EMD Millipore) followed by 30min in PBS. Heat-mediated antigen retrieval was performed by placing

slides in 1x sodium citrate buffer (PHR1416, Sigma), pH 6.0, and pulse-heated for 20min in the citrate buffer in the microwave. Slides were allowed to cool for 20min inside the microwave, followed by 30min at room temperature. Slides were then washed 3 times (15min each wash) in PBS and incubated in blocking solution for 1.5h at room temperature. Blocking solution contained 5% normal donkey serum (D9663, Sigma), 1% BSA (421501J, VWR), 0.1% Triton-X and 0.05% Tween-20 in PBS. Slices were incubated with monoclonal mouse anti-γH2A.X primary antibody (1:50; JBW301, Millipore) in 5% normal donkey serum and 1% BSA in PBS at 4°C overnight. On the following day, slides were further incubated for 30min at 37°C and washed 3 times in PBS (15min each wash). Slides were then incubated with 3% Sudan black solution in 70% ethanol for 10min at room temperature. After 3 rinses in $dH_2O$, slides were incubated with corresponding Alexa-conjugated secondary antibody (1:500; A21202, Thermo Fisher) diluted in 5% normal donkey serum in PBS for 1h at 37°C. Slides were then washed 3 times in PBS, followed by 3 times in $dH_2O$ (15min each wash). DAPI (D9542, Sigma) diluted 1:1,000 in PBS was subsequently applied for 10min and washed off with PBS (3 washes, 5min each). Sections were mounted in ProLong Gold antifade mountant (P36930, Thermo Scientific).

Immunocytochemistry and drug treatments

Pre-differentiated (day 2) LUHMES were plated down ($0.15x10^6$ cells per well) and grown on acid-etched coverslips, placed in 24-well plates and coated with PLO and fibronectin, followed by Geltrex (A1413201, Thermo Scientific). Day 14 LUHMES neurons were fixed with 4% PFA for 15min, rinsed with PBS and stored in TBS at 4°C until required. Neurons were permeabilised in 0.1% TBS-Triton X for 5min. Following three rinses with TBS, coverslips were incubated in blocking solution (5% normal donkey serum in 0.1% TBS- Tween) for 1h at room temperature and then overnight at 4°C with mouse monoclonal anti-γH2A.X primary antibody (1:400; JBW301, Millipore) and rabbit polyclonal anti-53BP1 primary antibody (1:1000, NB100304, Novus Biologicals) diluted in blocking solution. The next day, neurons were washed with 0.1% Tween-TBS (3x10min) and incubated with corresponding

secondary antibodies for 1h at room temperature. Secondary antibodies were Alexa Fluor 488-donkey anti-mouse IgG (1:300; A21202, Thermo Scientific) and Alexa Fluor 596-donkey anti-rabbit IgG (1:500; A21207, Thermo Scientific), and were diluted, together with DAPI (1:1,000; D9542, Sigma), in 4% normal donkey serum in 0.1% TBS- Tween. Cells were washed with TBS (3x10min) and mounted with ProLong Gold antifade mountant (P10144, Thermo Scientific). For the etoposide treatment experiments, LUHMES neurons were incubated with 0.5µM etoposide (E1383, Sigma) for 4h at 37°C prior to fixation.

Image acquisition and analysis

All imaging and counting procedures were performed blind to genotype. Image analysis was performed using the software package Fiji. Z-stacked confocal images, with a step size of 0.25µm (brain sections) or 1µm (LUHMES neurons), were acquired on a Nikon STORM/A1+ microscope at 60x (brain sections) or 100x (LUHMES neurons) magnification, using the NIS Elements software. The optimal laser intensity and gain that gave no signal in the no-primary antibody controls, were established and kept constant for all subsequent analyses. Three images of each region of interest were obtained from each mouse. The number of neurons with one or more γH2A.X-positive foci, as well as the total number of nuclei within a given area (approximately 200 nuclei on average) were counted manually and the percentage of γ-H2A.X-positive nuclei determined for each image. In the case of LUHMES neurons, nine independent wild-type and nine independent *SORCS2* knock-out lines were analysed. Approximately 100 nuclei (from four images belonging to different regions of the same coverslip) were counted for each line, and the number of γH2A.X/53BP1-positive foci per nucleus was calculated.

Quantitative reverse transcriptase PCR (qRT-PCR)

Cell pellets from day 14 LUHMES neurons were resuspended in RLT buffer (Qiagen) with 10% (v/v) 2-mercaptoethanol. Total RNA was extracted using the RNeasy mini kit (Qiagen), and 1µg per sample was reverse transcribed with Multiscribe Reverse Transcriptase using random hexamers in a 80µl

reaction. Controls, in which 25ng RNA of each sample was used to make cDNA in the absence of the Multiscribe Reverse Transcriptase, were included to detect genomic contamination.

PCR amplification of the cDNA obtained for each sample was quantified using the TaqMan® Universal PCR Mix No AmpErase® UNG (Life Technologies), and the threshold cycle (Ct) was determined using the Applied Biosystems 7900HT Fast Real-Time PCR System and the corresponding SDS software. TaqMan probes were used for the detection of *TOP2B* and eight reference genes (*CYC1*, *ERCC6*, *SDHA*, *TOP1*, *RPLPO*, *SCLY*, *TBP* and *UBE4A*). The GeNorm software was used to identify the most stably expressed reference genes (*SDHA* and *UBE4A*). A standard curve, generated from a dilution series, was run for *TOP2B* and the reference genes. The baseline and Ct values were determined for each gene and expression levels were calculated using the standard curve method for absolute quantification, where unknowns are compared to the generated standard curve and values are extrapolated. *TOP2B* expression values were subsequently normalised to the geometric mean of the reference genes.

Viability assay

Neuronal viability was assessed using the Alamar Blue assay (DAL1025, Thermo Scientific). This assay was chosen as: 1) it does not interfere with cell functioning and 2) it is not an end-point assay, i.e. it allows viability to be measured at multiple time points (Rampersad 2012). Viability was measured at day 6 and day 14 from an equivalent number of neurons ($0.25x10^6$) per line by replacing the medium with freshly made differentiation medium containing 10% (v/v) Alamar Blue solution. Cells were incubated with the Alamar Blue solution for 2h, after which the solution was transferred to a new 24-well plate and fluorescence measured in a FLUOstar OMEGA plate reader using an excitation wavelength of 540-570nm, and an emission wavelength of 580-610nm.

Statistical analysis

Statistical analyses were performed using GraphPad Prism. Differences between two means were assessed using unpaired Student's t-test, and among multiple means by one- or two-way ANOVA, followed by Tukey's, Sidak's or Dunnett's post hoc tests. Sample sizes were determined based on previously reported findings (Suberbielle et al 2013) or pilot experiments. Null hypotheses were rejected when $p<0.05$.

## Results

Our goals were to investigate i) whether we replicated the previous finding that exploration of a novel environment led to a temporary increase in the number of DSBs detected in the mouse brain and ii) whether deletion of *Sorcs2* in mice leads to higher levels of DSB formation upon exploration of a novel environment and/or a deficit in break repair (Fig. 1a). The novel environment paradigm comprised three groups of mice (5-6 months of age): those that a) remained in their home cage (baseline group); b) explored a novel environment (novel environment group) and c) explored a novel environment, followed by a recovery period in the home cage (recovery group), before they were sacrificed. As described previously (Suberbielle et al 2013), the proportion of neurons positive for γH2A.X (a widely used marker of DNA DSBs in neurons and other cell types) was determined in three brain regions (DG, CA2 and CA3 of the hippocampus, Suppl. Fig. 2; Suppl. Table 1). Two-way ANOVAs were performed for each brain region to assess the impacts of genotype and environment. In agreement with a previous report (Suberbielle et al 2013), exposing mice to a novel environment had a significant effect on the percentage of γH2A.X-positive nuclei detected in the DG and the CA2, while the result was marginal in the CA3 region of the hippocampus (DG: $F_{2,12} = 24.09$, $p < 0.0001$, CA2: $F_{2,12} = 7.122$, $p = 0.0091$, CA3: $F_{2,12} = 3.672$, $p= 0.0570$; Fig. 1b). Post-hoc analysis of the DG data obtained from the wild-type mice indicated that there were significantly more DSBs in the novel environment group compared to the baseline ($p < 0.0001$) and recovery ($p = 0.0025$) groups (Fig. 1b). In the CA2, the wild-type mice exposed to the novel environment also had significantly more DSBs

than the corresponding baseline group ($p = 0.0445$), but a significant difference was not seen in the novel environment versus recovery condition ($p = 0.1004$) (Fig. 1b). In contrast, there were no significant differences in the percentage of γH2A.X-positive nuclei across the three experimental groups in any of the brain regions examined in the *Sorcs2*$^{-/-}$ mice (DG: $F_{1,12} = 2.974$, $p = 0.1103$; CA2: $F_{1,12} = 0.6495$, $p = 0.4360$; CA3: $F_{1,12} = 1.224$, $p = 0.2902$). While no main effect of the genotype was observed in any region (DG: $p = 0.1103$; CA2: $p = 0.4360$; CA3: $p = 0.2902$), in the DG, we detected a significant genotype-environment interaction ($F_{2,12} = 8.19$, $p = 0.0057$). Visual inspection of the plotted data (Fig. 1b) suggested, and post-hoc analysis showed, that the genotype-environment interaction was driven by a greater number of breaks at baseline in the mutant compared to the wild-type group (Fig. 1b, $p = 0.0232$). Significant interactions were not observed in the CA2 ($F_{2,12} = 1.253$, $p = 0.3205$) or the CA3 ($F_{2,12} = 1.834$, $p = 0.2019$) regions for this or any other environmental comparison.

We next sought to replicate the finding of a higher number of breaks at baseline in the DG of the Sorcs2$^{-/-}$ mice using an independent set of age and sex-matched wild-type and *Sorcs2*$^{-/-}$ mice. As before, we detected significantly higher levels of DSBs in the *Sorcs2*$^{-/-}$ mice ($t_{10} = 2.786$, $p = 0.0193$; Fig. 1c).

Having determined that the *Sorcs2*$^{-/-}$ mice had higher levels of DNA DSBs at baseline we set out to determine whether this phenotype was also present in human neurons lacking *SORCS2*. We used CRISPR/Cas9 genome editing (Fig. 2a) to delete the gene in the human neuronal cell line, LUHMES, a karyotypically normal foetal mesencephalic cell line that can be robustly differentiated into post-mitotic dopaminergic neurons, with the majority of cells generating trains of spontaneous action potentials after 10-12 days of differentiation (Scholz et al 2011). Loss of *SORCS2* expression was shown by western blotting (Fig. 2b). Nine independent lines generated using two different gRNAs (four produced using a gRNA targeting exon 1 and five from the exon 3 gRNA) were used in all subsequent analyses.

To evaluate the effect of knocking out *SORCS2* on DNA DSB formation in human neurons, we stained untreated control (consisting of wild-type (WT) and empty vector (EV) lines) and *SORCS2* knock-out LUHMES neurons (day 14) for γH2A.X and 53BP1. The latter protein is quickly recruited to DSB sites, where it binds to γH2A.X and acts as a scaffold for the binding of additional DNA repair proteins from the non-homologous end joining (NHEJ) pathway, the main DNA repair pathway in post-mitotic cells (Firsanov et al 2011). As previously reported for neurons (Crowe et al 2006), more than 90% of the analysed neurons (wild-type and knock-out) had fewer than three double positive foci per nucleus, with the majority of nuclei having no foci (Figure 3A; top row). There was no significant difference in the number of foci per nucleus between control and *SORCS2* knock-out neurons ($t_{16}$ = 0.4664, p = 0.6472; Fig. 3b). No significant difference was observed also between the WT and EV lines ($t_7$ = 0.2396, p = 0.8175; Suppl. Fig. 3a), as well as between the *SORCS2* KOs generated by targeting exon 1 and exon 3 ($t_7$ = 0.293, p = 0.7780, Suppl. Fig. 3b). As DNA DSBs are rare, due to their dynamic repair, we next assessed whether *SORCS2* loss would have an effect on the number of DSBs following treatment with etoposide, which causes accumulation of Topoisomerase IIβ (TopoIIβ)-dependent DNA DSBs, by preventing their re-ligation through stabilisation of the TopoIIβ-DNA cleavable complex (Montecucco et al 2015). As expected, etoposide treatment greatly increased the number of DSBs per nucleus in both wild-type and *SORCS2* knock-out LUHMES neurons ($F_{1, 31}$ = 299, p < 0.0001; Fig. 3a [bottom row] and 3c) with the *SORCS2* knock-out lines having significantly more γH2A.X/53BP1-positive foci per nucleus than the wild-type lines (post-hoc p = 0.0355; Fig. 3c). There was no significant difference in the number of γH2A.X/53BP1-positive foci per nucleus between the *SORCS2* knock-out clones derived by targeting exon 1 and those generated by disrupting exon 3 ($t_7$ = 0.2139, p = 0.8367; Fig. 3d), or between the two control groups ($t_7$ = 0.2535, p = 0.8072, Suppl. Fig. 3b).

Treatment with etoposide had no impact on *TOP2B* expression ($F_{1, 16}$ = 0.9781, p = 0.8391, Suppl. Fig. 4). In addition, there was no significant difference in *TOP2B* levels between genotypes either prior to or following etoposide treatment ($F_{1, 16}$ = 2.652, p = 0.1230, Suppl. Fig. 4).

Given the link between neuronal activity and TopoIIβ-mediated DNA damage (Madabhushi et al 2015), we next investigated whether established paradigms of neuronal stimulation would have a differential impact on the formation of DNA DSBs in *SORCS2* knock-out and wild-type LUHMES neurons. First, we tested established neuronal activation agents, N-methyl-D-aspartate (NMDA), potassium chloride (KCl), and Glycine, in mature WT neurons to assess their effect on DSB generation in LUHMES. Brief treatments with NMDA (50µM) or KCl (10mM) had no effect on the number of γH2A.X/53BP1-positive foci per nucleus, while incubation with glycine (300µM) led to a significant increase in the number of DNA breaks ($p = 0.0001$, Suppl. Fig. 5). We next compared the impact of glycine treatment in control (WT and EV) and *SORCS2*$^{-/-}$ lines. No significant difference in the number of DNA DSB foci was observed between the two groups ($t_{14} = 0.3825$, $p = 0.7078$, Fig. 4).

Finally, given the negative impact of DSB formation on neuronal function and survival, we examined the effect of knocking out *SORCS2* on the overall neuronal viability both at early (day 6) and late (day 14) stages of differentiation. At day 6, there was no significant difference in the viability of wild-type neurons compared to that of the *SORCS2* knock-out clones ($t_{16} = 0.2958$, $p = 0.771$; Fig. 5a). However, at day 14, we detected a significant reduction in the viability of *SORCS2*$^{-/-}$ clones compared to controls ($t_{15} = 3.387$, $p = 0.004$; Fig. 5b).

## Discussion

We provide the first, to our knowledge, replication of a previous finding (Suberbielle et al 2013) that, in wild-type mice, exploration of a novel environment is associated with the acquisition of DNA DSBs, which are repaired after a recovery period. We found, however, no evidence to support our initial hypothesis that *Sorcs2* knock-out mice would show a greater number of breaks associated with the exploratory behaviour or impaired recovery from this experience. In contrast, somewhat surprisingly, we observed higher levels of DNA damage in the DG of *Sorcs2*$^{-/-}$ mice that remained in their home cage. We subsequently replicated this result in an independent set of knock-out and wild-type mice.

We next investigated whether higher levels of DNA damage would be also found in human neurons lacking *SORCS2*. DNA DSBs were rare in both mutant and wild-type lines, as has been reported previously for rat primary cortical neurons (Crowe et al 2006), and there was no detectable difference in γH2A.X immunoreactivity between the genotypes. As expected, treatment with the TopoIIβ inhibitor, etoposide, led to an increase in the number of breaks in both lines. The *SORCS2*$^{-/-}$ lines, however, had significantly more breaks following etoposide treatment. Despite the increased number of TopoIIβ-dependent breaks in the knock-out cell lines, there was no difference in *TOP2B* expression levels in mutant lines either before or after treatment with etoposide. As enhanced TopoIIβ activity and DSB levels have been observed following stimulation of neuronal activity (Madabhushi et al 2015), we next investigated whether stimulation of neuronal activity would lead to a differential response in the neurons lacking SORCS2. We found no evidence that loss of SORCS2 rendered the neurons more susceptible to neuronal activity-evoked DNA damage. This result is in keeping with our finding that *Sorcs2*$^{-/-}$ mice had a similar number of DNA DSBs to wild-type mice following exploration of a novel environment.

There are a number of potential explanations for the link between SORCS2 loss and DNA damage. Previous work (Malik et al 2019) implicated SorCS2 in protection against the oxidative stress-induced DNA damage and neuronal loss caused by a PTZ-induced kindling paradigm. Similarly, Smith *et al.* (2018) showed that *SORCS2* expression is stimulated by other stressors, such as alcohol and DEXA (Smith et al 2018). DEXA administration induces DNA damage, which can be prevented by application of reactive oxygen species (ROS) blockers (Ortega-Martínez 2015), thus SORCS2 loss may exacerbate the effect of cellular stressors on DNA damage and future experiments could test this hypothesis. Another possibility is that SORCS2 loss impacts the number of DNA DSBs, through loss of interaction with DNA repair proteins. SORCS2 has been shown to co-localise with the transactivation response DNA-binding protein of 43kDa (TDP-43) in ALS post-mortem brains (Miki et al 2018). TDP-43 is an RNA/DNA-binding protein that has recently been implicated in DSB repair (Mitra et al 2019). SORCS2 also interacts with Heterogeneous Nuclear Ribonucleoprotein U (hnRNP-U) (Fasci et al

459 2018). This DNA and RNA binding protein interacts with NEIL1, a DNA glycosylase implicated in the
460 repair of DNA damaged by reactive oxygen species, stimulating its base excision activity (Hegde et al
461 2012). Given the role of the VPS10P family in intracellular trafficking, future work could investigate
462 whether SORCS2 is involved in trafficking the above proteins.

463 While the cellular mechanism underlying the increase in DNA DSBs associated with SORCS2 loss is
464 still uncertain, it is of interest that mature (but not immature) *SORCS2*$^{-/-}$ neurons showed decreased
465 viability, in keeping with findings in mouse primary neurons lacking Sorcs2, which show higher rates
466 of apoptosis (independent of autophagy) when subject to lysosomal stressors (Almeida at al.,
467 submitted). The maintenance of genome integrity is very important, particularly for post-mitotic
468 long-lived cells, such as neurons, and DNA damage is linked to neurodegenerative disorders, ageing
469 and decreased expression of genes important for brain maintenance and function (Madabhushi et al
470 2015).

471 This study is subject to a number of limitations. An important factor is the small number of replicates
472 performed for the animal-based experiments, in particular. It is notable however that the set up was
473 sufficient to replicate Suberbielle et al.'s finding in wild-type mice undergoing the novel environment
474 task (Suberbielle et al 2013) and that we replicated the finding of increased numbers of breaks in the
475 mutant mice that remained in the home cage in an independent set of mice. It is also notable that
476 experiments performed in mice and a human cell line lacking SORCS2 showed consistent
477 phenotypes.

478 In summary, we have shown that SorCS2 loss in mice leads to higher levels of γH2A.X-positive DNA
479 breaks. Loss of SORCS2 in human neurons led to an increase in the number of TopoIIβ-dependent
480 breaks and decreased neuronal viability. Our findings in both species suggest that the impact of
481 SORCS2 loss is not mediated by a differing response to neuronal activation. An increase in DNA DSBs
482 may lead to an altered transcriptional profile, affect genome integrity and ultimately lead to cell
483 death. In agreement with this notion, DNA damage is increasingly being linked to cognitive

484 impairment, dementia and other neurodegenerative disorders (Mullaart et al 1990; Adamec et al
485 1999; Madabhushi et al 2014; Shanbhag et al 2019; Thadathil et al 2019), and attenuating the DNA
486 damage response to DSBs has been demonstrated to be protective in models of several
487 neurodegenerative disorders (Tuxworth et al 2019). Our findings are in keeping with the known
488 involvement of other sortilin family members in cognition, ageing and neurodegenerative disorders
489 and with the recent finding that SNPs in *SORCS2* are involved in epistatic interactions associated with
490 pathological hallmarks of Alzheimer's disease (Wang et al 2020). Future experimental work should
491 assess hypotheses based around SORCS2's role in the cellular response to stress and/or DNA repair
492 pathways.

493

494 **Abbreviations**

495 **53BP1:** p53-binding protein 1

496 **ADHD:** Attention deficit hyperactivity disorder

497 **ALS:** Amyotrophic lateral sclerosis

498 **BDNF:** Brain-derived neurotrophic factor

499 **BSA:** Bovine serum albumin

500 **Ct:** Cycle threshold

501 **DEXA:** Dexamethasone

502 **DG:** Dentate gyrus

503 **DSB:** Double-strand break

504 **EV:** Empty vector

505 **FACS:** Fluorescence-activated cell sorting

| | | |
|---|---|---|
| 506 | **GDNF:** | Glial cell-derived neurotrophic factor |
| 507 | **gRNA:** | Guide RNA |
| 508 | **GWAS:** | Genome-wide association study |
| 509 | **hnRNP-U:** | Heterogeneous nuclear ribonucleoprotein U |
| 510 | **KCl:** | Potassium chloride |
| 511 | **KO:** | Knock-out |
| 512 | **LTD:** | Long-term depression |
| 513 | **LTP:** | Long-term potentiation |
| 514 | **LUHMES:** | Lund human mesencephalic |
| 515 | **MSN:** | Medium spiny neurons |
| 516 | **NHEJ**: | Non-homologous end joining |
| 517 | **NMDAR:** | N-methyl-D-aspartate receptor |
| 518 | **PBS:** | Phosphate-buffered saline |
| 519 | **PLO:** | Poly-L-Ornithine |
| 520 | **PSD:** | Post-synaptic density |
| 521 | **PTZ:** | Pentylenetetrazol |
| 522 | **ROS:** | Reactive oxygen species |
| 523 | **SNP:** | Single-nucleotide polymorphism |
| 524 | **TBS:** | Tris-Buffered Saline |
| 525 | **TDP-43:** | Transactivation response DNA-binding protein of 43kDa |

526 **TH$^+$:** Tyrosine hydroxylase-positive

527 **TopoIIβ:** Topoisomerase IIβ

528 **TrkB:** Tropomyosin receptor kinase B

529 **Vps10p:** Vacuolar protein sorting (VPS) 10p

530 **VTA:** Ventral tegmental area

531 **WT:** Wild-type

532

533 **Acknowledgements**

534 We thank Dr Ian Adams for helpful discussions regarding scientific strategy and the manuscript
535 and Dr James Crichton for support with protocol optimisation and helpful comments on the
536 manuscript. KOG received salary support from an Alzheimer's Research UK award (ARUK-PPG2019B-
537 015) to KLE. TSJ is funded by the UK Dementia Research Institute which receives its funding from DRI
538 Ltd, funded by the UK Medical Research Council, Alzheimer's Society, and Alzheimer's Research UK,
539 and the European Research Council (ERC) under the European Union's Horizon 2020 research and
540 innovation programme (Grant agreement No. 681181).

541

542 **References**

543 **Adamec E, Vonsattel JP, Nixon RA (1999) DNA strand breaks in Alzheimer's disease. Brain Res**
544 **849:67–77. doi: 10.1016/s0006-8993(99)02004-1**

545 **Alemany S, Ribasés M, Vilor-Tejedor N, et al (2015) New suggestive genetic loci and biological**
546 **pathways for attention function in adult attention-deficit/hyperactivity disorder. Am J**
547 **Med Genet B, Neuropsychiatr Genet 168:459–470. doi: 10.1002/ajmg.b.32341**

548 **Crowe SL, Movsesyan VA, Jorgensen TJ, Kondratyev A (2006) Rapid phosphorylation of histone**
549 **H2A.X following ionotropic glutamate receptor activation. Eur J Neurosci 23:2351–2361.**
550 **doi: 10.1111/j.1460-9568.2006.04768.x**

551 **Davies G, Lam M, Harris SE, et al (2018) Study of 300,486 individuals identifies 148 independent**
552 **genetic loci influencing general cognitive function. Nat Commun 9:2098. doi:**
553 **10.1038/s41467-018-04362-x**

554 Deinhardt K, Kim T, Spellman DS, et al (2011) Neuronal growth cone retraction relies on
555 proneurotrophin receptor signaling through Rac. Sci Signal 4:ra82. doi:
556 10.1126/scisignal.2002060

557 Duncan L, Yilmaz Z, Gaspar H, et al (2017) Significant Locus and Metabolic Genetic Correlations
558 Revealed in Genome-Wide Association Study of Anorexia Nervosa. Am J Psychiatry
559 174:850–858. doi: 10.1176/appi.ajp.2017.16121402

560 Fabbri C, Serretti A (2016) Genetics of long-term treatment outcome in bipolar disorder. Prog
561 Neuropsychopharmacol Biol Psychiatry 65:17–24. doi: 10.1016/j.pnpbp.2015.08.008

562 Fabbri C, Tansey KE, Perlis RH, et al (2018) New insights into the pharmacogenomics of
563 antidepressant response from the GENDEP and STAR*D studies: rare variant analysis and
564 high-density imputation. Pharmacogenomics J 18:413–421. doi: 10.1038/tpj.2017.44

565 Fasci D, van Ingen H, Scheltema RA, Heck AJR (2018) Histone interaction landscapes visualized by
566 crosslinking mass spectrometry in intact cell nuclei. Mol Cell Proteomics 17:2018–2033.
567 doi: 10.1074/mcp.RA118.000924

568 Firsanov DV, Solovjeva LV, Svetlova MP (2011) H2AX phosphorylation at the sites of DNA double-
569 strand breaks in cultivated mammalian cells and tissues. Clin Epigenetics 2:283–297. doi:
570 10.1007/s13148-011-0044-4

571 Glerup S, Bolcho U, Mølgaard S, et al (2016) SorCS2 is required for BDNF-dependent plasticity in
572 the hippocampus. Mol Psychiatry 21:1740–1751. doi: 10.1038/mp.2016.108

573 Glerup S, Nykjaer A, Vaegter CB (2014a) Sortilins in neurotrophic factor signaling. Handb Exp
574 Pharmacol 220:165–189. doi: 10.1007/978-3-642-45106-5_7

575 Glerup S, Olsen D, Vaegter CB, et al (2014b) SorCS2 regulates dopaminergic wiring and is processed
576 into an apoptotic two-chain receptor in peripheral glia. Neuron 82:1074–1087. doi:
577 10.1016/j.neuron.2014.04.022

578 Greenwood TA, Lazzeroni LC, Maihofer AX, et al (2019) Genome-wide Association of
579 Endophenotypes for Schizophrenia From the Consortium on the Genetics of Schizophrenia
580 (COGS) Study. JAMA Psychiatry 76:1274–1284. doi: 10.1001/jamapsychiatry.2019.2850

581 Hegde ML, Banerjee S, Hegde PM, et al (2012) Enhancement of NEIL1 protein-initiated oxidized
582 DNA base excision repair by heterogeneous nuclear ribonucleoprotein U (hnRNP-U) via
583 direct interaction. J Biol Chem 287:34202–34211. doi: 10.1074/jbc.M112.384032

584 Hermey G (2009) The Vps10p-domain receptor family. Cell Mol Life Sci 66:2677–2689. doi:
585 10.1007/s00018-009-0043-1

586 Karlsson Linnér R, Biroli P, Kong E, et al (2019) Genome-wide association analyses of risk tolerance
587 and risky behaviors in over 1 million individuals identify hundreds of loci and shared
588 genetic influences. Nat Genet 51:245–257. doi: 10.1038/s41588-018-0309-3

589 Lotharius J, Barg S, Wiekop P, et al (2002) Effect of mutant alpha-synuclein on dopamine
590 homeostasis in a new human mesencephalic cell line. J Biol Chem 277:38884–38894. doi:
591 10.1074/jbc.M205518200

592 Ma Q, Yang J, Milner TA, et al (2017) SorCS2-mediated NR2A trafficking regulates motor deficits in
593 Huntington's disease. JCI Insight. doi: 10.1172/jci.insight.88995

Madabhushi R, Gao F, Pfenning AR, et al (2015) Activity-Induced DNA Breaks Govern the Expression of Neuronal Early-Response Genes. Cell 161:1592–1605. doi: 10.1016/j.cell.2015.05.032

Madabhushi R, Pan L, Tsai L-H (2014) DNA damage and its links to neurodegeneration. Neuron 83:266–282. doi: 10.1016/j.neuron.2014.06.034

Malik AR, Szydlowska K, Nizinska K, et al (2019) SorCS2 Controls Functional Expression of Amino Acid Transporter EAAT3 and Protects Neurons from Oxidative Stress and Epilepsy-Induced Pathology. Cell Rep 26:2792–2804.e6. doi: 10.1016/j.celrep.2019.02.027

Miki Y, Mori F, Seino Y, et al (2018) Colocalization of Bunina bodies and TDP-43 inclusions in a case of sporadic amyotrophic lateral sclerosis with Lewy body-like hyaline inclusions. Neuropathology 38:521–528. doi: 10.1111/neup.12484

Mitra J, Guerrero EN, Hegde PM, et al (2019) Motor neuron disease-associated loss of nuclear TDP-43 is linked to DNA double-strand break repair defects. Proc Natl Acad Sci USA 116:4696–4705. doi: 10.1073/pnas.1818415116

Montecucco A, Zanetta F, Biamonti G (2015) Molecular mechanisms of etoposide. EXCLI J 14:95–108. doi: 10.17179/excli2015-561

Mullaart E, Boerrigter ME, Ravid R, et al (1990) Increased levels of DNA breaks in cerebral cortex of Alzheimer's disease patients. Neurobiol Aging 11:169–173. doi: 10.1016/0197-4580(90)90542-8

Olsen D, Kaas M, Lundhede J, et al (2019) Reduced alcohol seeking and withdrawal symptoms in mice lacking the BDNF receptor sorcs2. Front Pharmacol 10:499. doi: 10.3389/fphar.2019.00499

Olsen D, Wellner N, Kaas M, et al (2021) Altered dopaminergic firing pattern and novelty response underlie ADHD-like behavior of SorCS2-deficient mice. Transl Psychiatry 11:74. doi: 10.1038/s41398-021-01199-9

Ortega-Martínez S (2015) Dexamethasone acts as a radiosensitizer in three astrocytoma cell lines via oxidative stress. Redox Biol 5:388–397. doi: 10.1016/j.redox.2015.06.006

Rampersad SN (2012) Multiple applications of Alamar Blue as an indicator of metabolic function and cellular health in cell viability bioassays. Sensors (Basel) 12:12347–12360. doi: 10.3390/s120912347

Scholz D, Pöltl D, Genewsky A, et al (2011) Rapid, complete and large-scale generation of post-mitotic neurons from the human LUHMES cell line. J Neurochem 119:957–971. doi: 10.1111/j.1471-4159.2011.07255.x

Shanbhag NM, Evans MD, Mao W, et al (2019) Early neuronal accumulation of DNA double strand breaks in Alzheimer's disease. Acta Neuropathol Commun 7:77. doi: 10.1186/s40478-019-0723-5

Smith AH, Ovesen PL, Skeldal S, et al (2018) Risk locus identification ties alcohol withdrawal symptoms to SORCS2. Alcohol Clin Exp Res 42:2337–2348. doi: 10.1111/acer.13890

Suberbielle E, Sanchez PE, Kravitz AV, et al (2013) Physiologic brain activity causes DNA double-strand breaks in neurons, with exacerbation by amyloid-β. Nat Neurosci 16:613–621. doi: 10.1038/nn.3356

635 **Thadathil N, Hori R, Xiao J, Khan MM (2019) DNA double-strand breaks: a potential therapeutic**
636 **target for neurodegenerative diseases. Chromosome Res 27:345–364. doi:**
637 **10.1007/s10577-019-09617-x**

638 **Tuxworth RI, Taylor MJ, Martin Anduaga A, et al (2019) Attenuating the DNA damage response to**
639 **double-strand breaks restores function in models of CNS neurodegeneration. Brain**
640 **Commun 1:fcz005. doi: 10.1093/braincomms/fcz005**

641 **Wang H, Yang J, Schneider JA, et al (2020) Genome-wide interaction analysis of pathological**
642 **hallmarks in Alzheimer's disease. Neurobiol Aging 93:61–68. doi:**
643 **10.1016/j.neurobiolaging.2020.04.025**

644 **Yang J, Ma Q, Dincheva I, et al (2020) SorCS2 is required for social memory and trafficking of the**
645 **NMDA receptor. Mol Psychiatry. doi: 10.1038/s41380-020-0650-7**

646

647

## 648 Figure Legends

649 **Fig. 1** Exploration of a novel environment is associated with a transient increase in DSBs in the
650 dentate gyrus and the CA2. (a) Experimental design. WT and Sorcs2-/- mice were divided into three
651 groups: 'home cage' (white), 'Novel E' (novel environment; light grey) and 'recovery' (dark grey). (b)
652 For each brain region, the percentages of γH2A.X-positive nuclei was calculated in 5-6 month-old WT
653 (open bars) and Sorcs2$^{-/-}$ mice (dotted bars) belonging to one of the three experimental groups.
654 Three brain sections per region per mouse, n=3 per experimental group. *p<0.05; **p<0.01;
655 ****p<0.0001 (Two-way ANOVA, followed by Tukey's multiple comparisons test). (c) Percentage of
656 nuclei positive for γH2A.X in the DG of wild-type (open bars) and Sorcs2$^{-/-}$ (dotted bars) mice in a
657 replication study. Three brain sections per region per mouse, n=7-5. *p<0.05 (unpaired Student's t-
658 test). Error bars represent means ± SEM Error bars represent means ± SEM

659 **Fig. 2** Strategy for knocking out *SORCS2* in LUHMES using CRISPR/Cas9 genome editing. (a)
660 Experimental design of the CRISPR/Cas9 experiments. gRNA sequences (underlined) within *SORCS2*
661 exon 1 and exon 3 used (separately) to knock out the gene using CRISPR/Cas9 genome editing.
662 Created with BioRender.com. (b) Representative western blots show a complete loss of SORCS2 in
663 the KO clones after targeting exon 1 (n=4 independent cell lines) or exon 3 (n=5 independent lines)

664 **Fig. 3** Knocking out *SORCS2* leads to increased TopoIIβ-dependent DSB formation in LUHMES
665 neurons. (a) Representative confocal images from untreated (top row) and etoposide-treated
666 (bottom row) WT and *SORCS2* KO LUHMES neurons (day 14) immunostained with γH2A.X (green)
667 and 53BP1 (red), and counterstained with DAPI (blue). White arrows point towards γH2A.X/53BP1
668 dual positive foci, and red- towards foci positive for γH2A.X only. Images were taken at 100x
669 magnification; scale bars: 10 µm. (b) Number of DSBs (γH2A.X/53BP1-positive foci) per nucleus in
670 untreated WT (white bar) and *SORCS2* KO (grey bar) LUHMES neurons (day 14); n= 8- 9 independent
671 cell lines per genotype. Unpaired Student's t-test. (c) Number of DSBs (γH2A.X/53BP1-positive foci)
672 per nucleus in etoposide-treated (dotted bars) compared to untreated (open bars) WT (white bars)
673 and *SORCS2* KO (grey bars) LUHMES neurons (day 14); n=9 independent lines per genotype. *p<0.05;
674 ****p<0.0001 (Two-way ANOVA, followed by Sidak's multiple comparisons test). (d) Number of
675 DSBs (γH2A.X/53BP1-positive foci) per nucleus in etoposide-treated *SORCS2* KO LUHMES neurons
676 (day 14) generated by targeting exon 1 (n=4 independent cell lines) or exon 3 (n=5 independent cell
677 lines). Unpaired Student's t-test. Approximately 100 nuclei counted per cell line; error bars represent
678 means ± SEM

679 **Fig. 4** Treatment with Glycine has no differential effect on DNA DSB formation in *SORCS2* KO
680 LUHMES neurons. No significant difference in the number of DSBs (γH2A.X/53BP1-positive foci) per
681 nucleus was identified between WT (white bar) and *SORCS2* KO (grey bar) LUHMES neurons (day 14)
682 following treatment with Glycine. N = 8 independent cell lines per genotype. Unpaired Student's t-
683 test

684 **Fig. 5** Knocking out *SORCS2* is associated with decreased neuronal viability at late (day 14), but not
685 early (day 6) stages of neuronal differentiation. Neuronal viability of WT (white bar) and *SORCS2* KO
686 (grey bar) LUHMES neurons measured at early (day 6) (a) and late (day 14) (b) stages of
687 differentiation. **p<0.01 (unpaired Student's t-test); Error bars represent means ± SEM; n=8-9
688 independent cell lines per genotype

689 **Suppl. Fig. 1** Schematic representation of the areas of the hippocampus immunostained for γH2A.X
690 and counterstained with DAPI. Three 14µm thick sections were obtained at intervals of 700µm,
691 starting from the first section in which all regions of the hippocampus (i.e. CA1, CA2 and CA3) was
692 visible. This corresponds to bregmas -1.755, -2.155 and -2.555. Confocal images were obtained
693 within the DG, CA2 and CA3 regions as indicated by boxes A, B and C, respectively. Created with
694 BioRender.com

695 **Suppl. Fig. 2** DSB formation in WT and *Sorcs2*$^{-/-}$ mice at baseline, following exploratory activity and
696 recovery in the home cage. Single planes from the maximum projections of representative confocal
697 images taken from the DG of WT (top row) and *Sorcs2*$^{-/-}$ (bottom row) mice belonging to one of the
698 three experimental conditions- home cage (left column), novel environment (middle column) and
699 recovery (right column). γH2A.X-positive foci (green) were localised within nuclei (blue). When
700 counting positive nuclei, due to the high nuclei density, each plane was examined individually. The
701 nuclei positive for γH2A.X in each plane were marked while counting to avoid oversampling. White
702 and red arrows point towards γH2A.X-positive and negative nuclei, respectively. 60x magnification;
703 scale bars: 10µm

704 **Suppl. Fig. 3** DSB formation in WT and *SORCS2* KO LUHMES neurons. Number of DSBs
705 (γH2A.X/53BP1-positive foci) per nucleus in untreated (a) and etoposide-treated (b) WT (n= 6
706 independent cell lines) and EV (n= 3 independent cell lines) LUHMES neuron day 14. (c) Number of
707 DSBs (γH2A.X/53BP1-positive foci) per nucleus in untreated *SORCS2* KO LUHMES neurons (day 14)
708 generated by targeting exon 1 (n=4 independent cell lines) or exon 3 (n=5 independent cell lines).
709 Unpaired Student's t-test. Approximately 100 nuclei counted per cell line. Error bars represent
710 means ± SEM

711 **Suppl. Fig. 4** Knocking out *SORCS2* has no effect on *TOP2B* expression levels. *TOP2B* expression levels
712 in untreated (open bars) and etoposide-treated (dotted bars) WT and *SORCS2* KO LUHMES neurons
713 (day 14). *TOP2B* expression was normalised to the expression of two reference genes- *SDHA* and

714 *UBE4A*; No significant effect of the treatment ($F_{2,16}$ = 0.9781, p = 0.3374), the genotype ($F_{2,16}$ = 2.652,
715 p = 0.1230) or the interaction between the two ($F_{2,16}$ = 0.0426, p= 0.8391) was identified (Two-way
716 ANOVA). N= 4-6 independent WT and *SORCS2* KO lines, respectively; error bars represent means ±
717 SEM

718 **Suppl. Fig. 5** Glycine treatment is associated with increased DSB formation in LUHMES neurons.
719 Number of DSBs (γH2A.X/53BP1-positive foci) per nucleus in untreated, NMDA, KCl or Glycine
720 treated WT LUHMES neurons (day 14). Cells were treated with: NMDA (50µM) for 10 min, followed
721 by a 10min recovery in differentiation media or for 30min without recovery (NMDA'); KCl (10mM)
722 for 20 min; Glycine (300µM) in $Mg^{2+}$ free ACSF for 5min, followed by 15min recovery in ACSF with
723 $Mg^{2+}$. ****p<0.0001 (One-way ANOVA, followed Dunnett's multiple comparisons test). N = 2-3
724 independent WT lines, approximately 100 nuclei counted per cell line. Error bars represent means ±
725 SEM

726

727 **Suppl. Table 1** Mean and standard deviation of the percentage γH2A.X-positive neurons in the DG,
728 the CA2 and CA3 region of the hippocampus of wild-type and *Sorcs2*$^{-/-}$ mice belonging to one of the
729 three experimental groups- home cage, novel environment and recovery

| Condition | Dentate gyrus | | CA2 | | CA3 | |
|---|---|---|---|---|---|---|
| | Mean % | Standard deviation | Mean % | Standard deviation | Mean % | Standard deviation |
| **Wild-type mice** | | | | | | |
| **Home cage** | 34.25938 | 3.951661 | 33.78725 | 6.976048 | 40.67963 | 10.46187 |
| **Novel environment** | 58.04647 | 2.134649 | 57.94746476 | 3.457886 | 58.03865 | 4.167395 |
| **Recovery** | 41.73074 | 1.907175 | 34.57381 | 5.601357 | 38.47548 | 8.155732 |
| ***Sorcs2*$^{-/-}$ mice** | | | | | | |
| **Home cage** | 46.31996 | 3.340785 | 40.51054 | 14.16338 | 52.21577 | 5.153943 |
| **Novel environment** | 52.01193 | 4.919772 | 51.62685 | 4.597567 | 52.00494 | 1.386886 |
| **Recovery** | 45.15117 | 0.915894 | 39.75985 | 13.88005 | 46.00351 | 7.454623 |

730

731

732

733

**Figure 1**

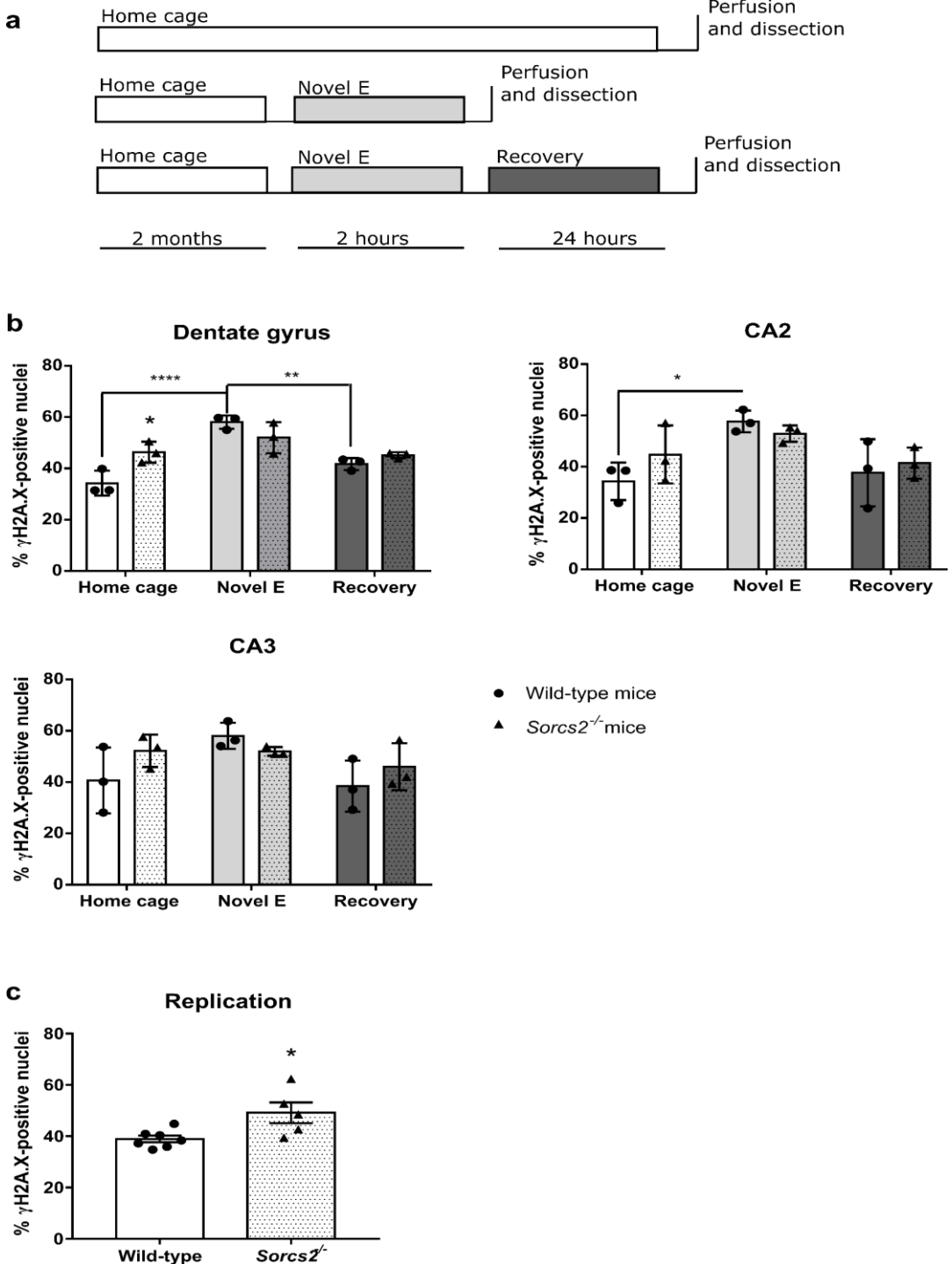
a
Home cage
Perfusion and dissection
Home cage
Novel E
Perfusion and dissection
Home cage
Novel E
Recovery
Perfusion and dissection
2 months
2 hours
24 hours
b
Dentate gyrus
CA2
CA3
% γH2A.X-positive nuclei
Home cage
Novel E
Recovery
Wild-type mice
Sorcs2-/- mice
c
Replication
Wild-type
Sorcs2-/-

**Figure 2**

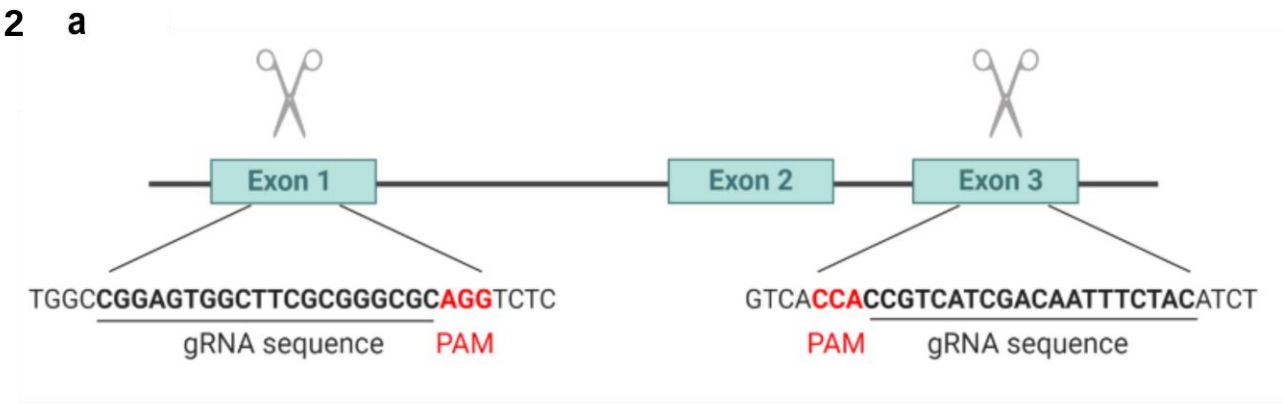
a
Exon 1
Exon 2
Exon 3
TGGCCGGAGTGGCTTCGCGGGCGCAGGTCTC
gRNA sequence
PAM
GTCACCACCGTCATCGACAATTTCTACATCT
PAM
gRNA sequence

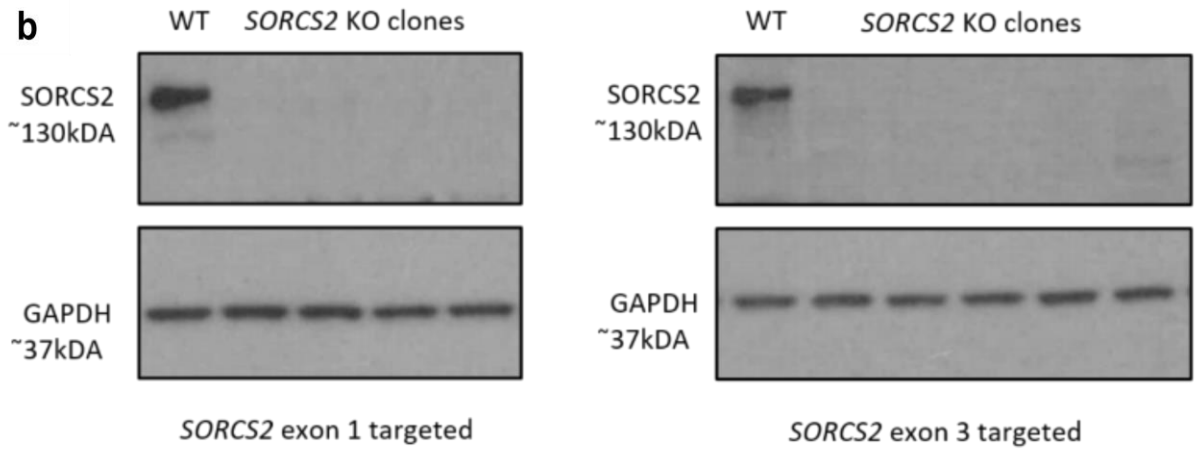
b
WT
SORCS2 KO clones
SORCS2
~130kDA
GAPDH
~37kDA
SORCS2 exon 1 targeted
WT
SORCS2 KO clones
SORCS2
~130kDA
GAPDH
~37kDA
SORCS2 exon 3 targeted

**Figure 3**

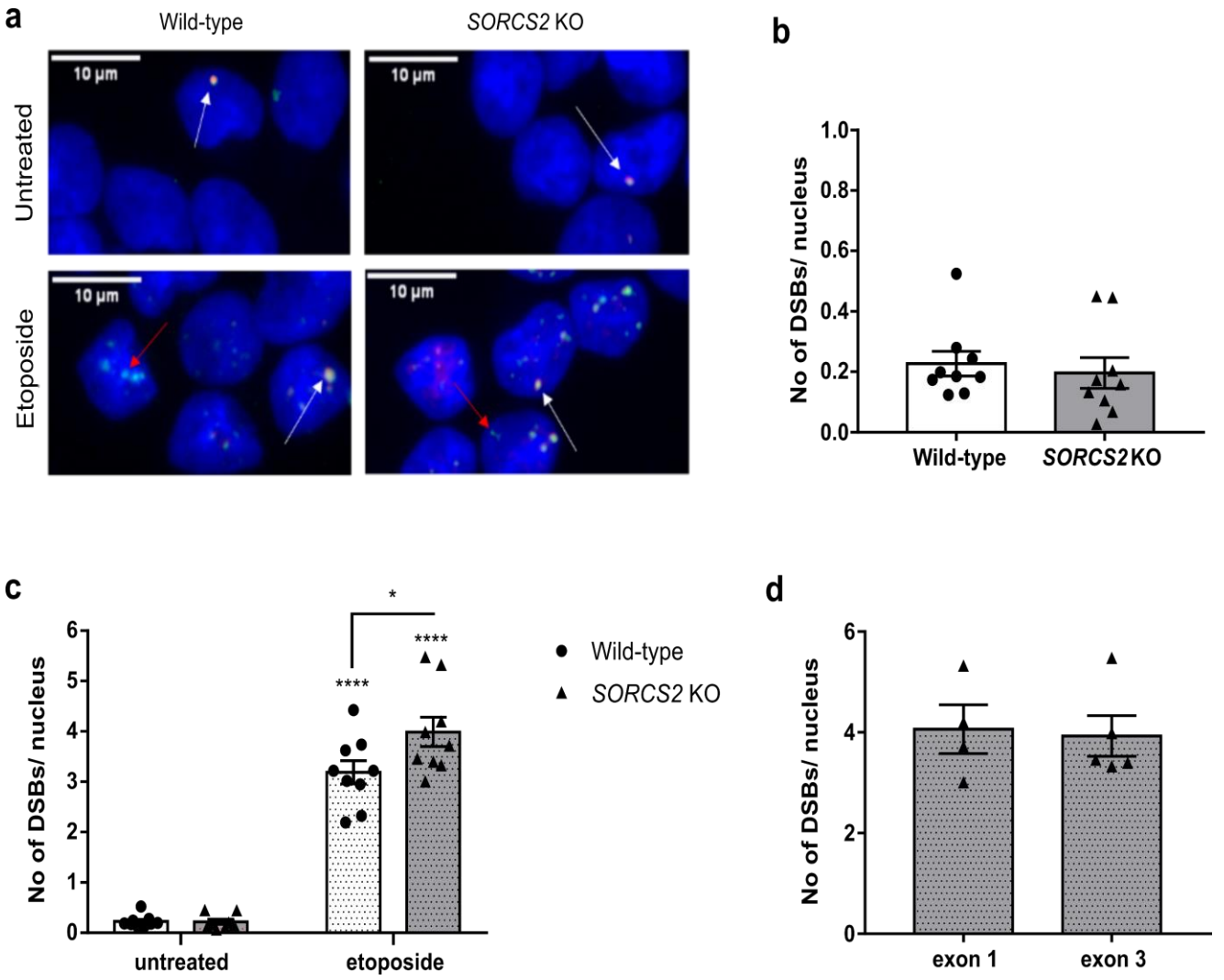
a
Wild-type
SORCS2 KO
Untreated
Etoposide
10 µm
b
No of DSBs/ nucleus
1.0
0.8
0.6
0.4
0.2
0.0
Wild-type
SORCS2KO
c
No of DSBs/ nucleus
6
5
4
3
2
1
0
****
****
*
untreated
etoposide
Wild-type
SORCS2 KO
d
No of DSBs/ nucleus
6
4
2
0
exon 1
exon 3

**Figure 4**

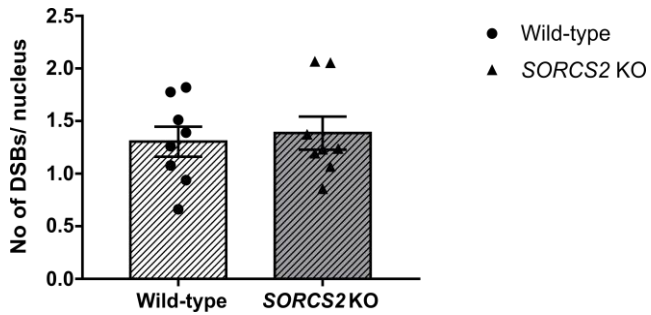
No of DSBs/ nucleus
2.5
2.0
1.5
1.0
0.5
0.0
Wild-type
SORCS2 KO
Wild-type
SORCS2 KO

Figure 5 a

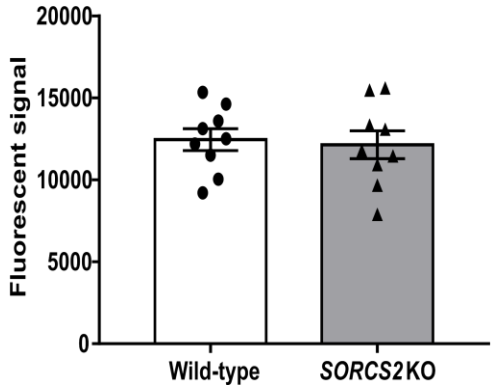
20000
15000
10000
5000
0
Fluorescent signal
Wild-type
SORCS2KO

b

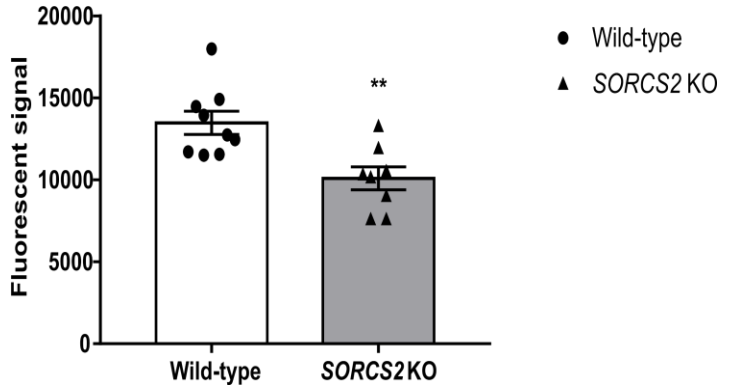
20000
15000
10000
5000
0
Fluorescent signal
**
Wild-type
SORCS2KO
Wild-type
SORCS2 KO